

On the galaxy–halo connection in the EAGLE simulation

Harry Desmond^{1,2}*, Yao-Yuan Mao^{3,4}, Risa H. Wechsler^{1,2}, Robert A. Crain⁵, and Joop Schaye⁶

¹*Kavli Institute for Particle Astrophysics and Cosmology, Physics Department, Stanford University, Stanford, CA 94305, USA*

²*SLAC National Accelerator Laboratory, Menlo Park, CA 94025, USA*

³*Department of Physics and Astronomy, University of Pittsburgh, Pittsburgh, PA 15260, USA*

⁴*Pittsburgh Particle Physics, Astrophysics, and Cosmology Center (PITT PACC), Pittsburgh, PA 15260, USA*

⁵*Astrophysics Research Institute, Liverpool John Moores University, 146 Brownlow Hill, Liverpool, L3 5RF, UK*

⁶*Leiden Observatory, Leiden University, P.O. Box 9513, 2300 RA Leiden, the Netherlands*

19 July 2022

ABSTRACT

Empirical models of galaxy formation require assumptions about the correlations between galaxy and halo properties. These may be calibrated against observations or inferred from more detailed physical models, such as hydrodynamical simulations. In this *Letter*, we use the EAGLE simulation to investigate the correlation of galaxy size with halo properties. We motivate this analysis by noting that the common assumption of angular momentum partition between baryons and dark matter in the local universe overpredicts both the spread in the stellar mass–size relation and the anticorrelation of size and velocity residuals, indicating a problem with the galaxy–halo connection it implies. We find the EAGLE galaxy population to perform significantly better with regard to both statistics, and trace this success to the weakness of the correlations of galaxy size with dark matter mass, concentration and spin at fixed stellar mass. Using these correlations in empirical models will enable fine-grained aspects of galaxy scaling relations to be matched.

Key words: galaxies: formation – galaxies: fundamental parameters – galaxies: haloes – galaxies: kinematics and dynamics – galaxies: statistics – dark matter

1 INTRODUCTION

Accurate semi-analytic and empirical modelling of galaxy formation is challenging, in part because the correlations of key galaxy and halo variables remain unknown. Observational manifestations of these correlations include galaxy scaling relations, and through detailed investigations of these relations we may hope to build knowledge of the galaxy–halo connection.

Over the past decades, two models which have proven useful for capturing aspects of the galaxy–halo connection are abundance matching (AM; Kravtsov et al. 2004; Behroozi et al. 2010), and the angular momentum partition model of Mo, Mao & White (1998, hereafter MMW). The former asserts a nearly monotonic relationship between stellar mass and a halo proxy, essentially establishing the dependence of galaxy mass on halo mass and concentration required to reproduce observations of galaxies’ clustering and dynamics (e.g. Conroy, Wechsler & Kravtsov 2006; Trujillo-Gomez et al. 2011; Reddick et al. 2013; Lehmann et al. 2015). The latter imposes a proportionality between galaxy and halo specific angular momentum, making galaxy size a function of galaxy mass and halo mass, concentration and spin. This yields good agreement with ob-

served average galaxy sizes over a wide range of mass (Kravtsov 2013; Desmond & Wechsler 2015, hereafter DW15).

Despite these successes, however, the conjunction of these models (hereafter “AM+MMW”) is known to make incorrect predictions for two properties of the galaxy population. The first is the scatter s_{MSR} in the stellar mass–size relation (MSR; de Jong & Lacey 2000; Gnedin et al. 2007). Angular momentum partition sets galaxy size proportional to halo spin, λ , and hence requires the scatter in size at fixed mass to be at least as large as that in λ . In fact, these scatters are ~ 0.2 dex and ~ 0.25 dex in observed galaxies and simulations respectively (DW15). The second is the correlation of residuals of the mass–size and mass–velocity relations ($\rho_{\Delta R-\Delta V}$), which is negligible in observations but predicted to be negative (McGaugh 2005; Dutton et al. 2007; DW15). These discrepancies indicate that the galaxy–halo correlations on which s_{MSR} and $\rho_{\Delta R-\Delta V}$ depend are inadequately captured by AM+MMW.

This issue is relevant also for semi-analytic models. Many such models set galaxy size proportional to halo virial radius (e.g. Somerville et al. 2008; Croton et al. 2006; Lu et al. 2011), sometimes with a single value for all halo spins. Others that use additional physical assumptions find important correlations of size with variables beyond halo mass and spin, but neglect the scatter in sizes (e.g. Lu, Mo & Wechsler 2015). The empirical identification

* E-mail: harryd2@stanford.edu

of the aspects of the galaxy–halo connection responsible for realistic size distributions – and correlations with velocity – will be of use in constraining such models and guiding the choice of inputs.

The failure of AM+MMW may be due either to inaccuracies in the properties of the halo populations on which the models were based (e.g. their neglect of baryonic physics), or incorrect prediction of the models themselves for the galaxy–halo connection. To resolve this dilemma, we turn in this *Letter* to hydrodynamical simulations, which enable the prediction of galaxy properties without prior assumptions on galaxy–halo correlations. In particular, we investigate s_{MSR} and $\rho_{\Delta R - \Delta V}$ in the EAGLE simulation (Schaye et al. 2015; Crain et al. 2015),¹ which has been shown to match the galaxy size distribution as well as many other aspects of galaxy phenomenology (Furlong et al. 2015). Sales et al. (2009) and Stevens et al. (2016) have previously shown that the MMW model fails to match the output of the EAGLE simulation and its ancestor OWLS. Zavala et al. (2016) found the angular momentum of stars to correlate with that of the inner halo in EAGLE, Sales et al. (2012) reported weak correlation of galaxy properties with halo spin in the related GIMIC simulation, and Ferrero et al. (2016) studied the EAGLE Tully–Fisher and mass–size relations.

The structure of this paper is as follows. In Section 2 we describe the EAGLE simulation and our methods to measure and explore the origin of s_{MSR} and $\rho_{\Delta R - \Delta V}$. In Section 3.1 we show that both s_{MSR} and $\rho_{\Delta R - \Delta V}$ are significantly nearer to their observed values in EAGLE than predicted by the AM+MMW model, and close to the predictions of AM alone. We show the success of EAGLE over AM+MMW to be due not to differences in underlying halo properties caused by baryons (Section 3.2), but rather to the correlations of halo variables with galaxy size (Section 3.3). In EAGLE, the sizes of low-redshift galaxies are only weakly correlated at fixed stellar mass with the mass, concentration and spin of their haloes, violating the assumption of angular momentum partition. Section 4 discusses the broader implications of these results, and summarises.

2 SIMULATIONS AND METHODS

2.1 The EAGLE simulation

EAGLE is a recently completed set of cosmological hydrodynamical simulations, run with a modified version of GADGET-3 (Springel 2005) and including hydrodynamics, radiative cooling, star formation, stellar feedback and black hole dynamics. The subgrid models were calibrated against the present-day stellar mass function and the normalisation of the mass–size relation. The simulations used a flat Λ CDM cosmology with $\Omega_m = 0.307$, $\Omega_b = 0.04825$, $h = 0.6777$, $\sigma_8 = 0.8288$ and $n_s = 0.9611$. We analyse the $z = 0$ snapshot of simulation Ref-L100N1504, which tracks 1504^3 dark matter and gas particles from $z = 127$ to the present day in a box with comoving side length 100 Mpc, in addition to the corresponding dark matter only (DMO) run in which baryonic effects were switched off. We refer the reader to Schaye et al. (2015) and Crain et al. (2015) for further information about the simulation.

2.2 Finding and matching haloes

To enable direct comparison with the results of DW15, we perform halo finding on both the DMO and hydrodynamical (hereafter ‘‘hydro’’) runs of the EAGLE simulation using ROCKSTAR (Behroozi

et al. 2013). We define spin as $\lambda \equiv J|E|^{1/2}G^{-1}M^{-5/2}$, where J is a halo’s angular momentum and E its total energy (Peebles 1969), and calculate concentration (c) using $r_{s, \text{klypin}}$ (derived from $V_{\text{max}}/V_{\text{vir}}$; Klypin et al. 2001) rather than fitting an NFW profile. We include only dark matter when calculating c and λ . We multiply the DMO haloes’ virial masses by $1 - \Omega_b/\Omega_m$ to compare to the hydro haloes, where again we include dark matter only (M_{DM}).

Next, we match the DMO ROCKSTAR catalogue to both the hydro ROCKSTAR catalogue and the SUBFIND catalogue (Springel et al. 2001; Dolag et al. 2009) made by the EAGLE pipeline, as follows. Both halo finders produce a list of particles associated with each halo that they identify. Since the two runs share the same dark matter particle IDs, we can match the haloes by finding common particles. In practice, given a halo in the DMO run (halo A), we first find the halo (halo B) in the hydro run that contains the most particles of halo A. If halo A also contains the most particles of halo B, we identify a ‘‘match’’ between them. Since the SUBFIND catalogue of the hydro run also provides the connection between the haloes and galaxies, this method establishes a link between the haloes in the DMO and hydro ROCKSTAR catalogues, and the galaxies in the SUBFIND catalogue. The fraction of haloes in the hydro run hosting galaxies with $M_* > 10^9 M_\odot$ that are matched by our procedure is 91 per cent; these haloes are not significantly biased in M_{DM} , c or λ .

2.3 Statistics

For both the data and models, we take s_{MSR} to be the Gaussian scatter in radius of the best-fitting power-law relation² between stellar mass (M_*) and half-mass radius (R_{eff} ; measured for stars in a 30 kpc aperture), over the range $9 < \log(M_*/M_\odot) < 11.5$. We have verified that restricting to $\log(M_*/M_\odot) > 10$ does not affect our conclusions. We measure $\rho_{\Delta R - \Delta V}$ as the Spearman rank correlation coefficient of the $\Delta R_{\text{eff}} - \Delta V_{\text{max}}$ relation, where Δx denotes the residual of quantity $\log(x)$ after subtracting the value expected at that M_* given a power-law fit to the $\log(M_*) - \log(x)$ relation, $f_x(M_*)$:

$$\Delta x \equiv \log(x) - f_x(M_*). \quad (1)$$

We quantify the dependence of R_{eff} on halo variables with the Spearman correlation coefficients $\rho_{\Delta R - \Delta X}$, where $X \in \{M_{\text{DM}}, c, \lambda\}$. We record in Table 1 the median and 1σ spread of the statistics over 100 Monte Carlo mock data sets of galaxies with M_* values within 0.01 dex of those of the observational sample (see Section 3.1).

3 RESULTS

3.1 The EAGLE mass–size and $\Delta R - \Delta V$ relations

Figure 1a shows the MSR of the EAGLE galaxies, and Figure 1b the correlation of their size and velocity residuals. We compare to the data of Pizagno et al. (2007, P07) to promote compatibility with DW15, although many studies find similar results (Verheijen 2001; McGaugh 2005; Courteau et al. 2007; Reyes et al. 2011). That both EAGLE relations are in approximate agreement with the observations is verified quantitatively in the first two rows of Table 1, which list the s_{MSR} and $\rho_{\Delta R - \Delta V}$ values.

The 3rd and 4th columns of Table 1 show analogous results

² Note that the use of a power law in this definition means that s_{MSR} is increased by curvature in the MSR; thus s_{MSR} for the EAGLE relation (see Fig. 1a) may be considered an upper bound on the ‘‘true’’ intrinsic scatter.

¹ <http://eagle.strw.leidenuniv.nl>

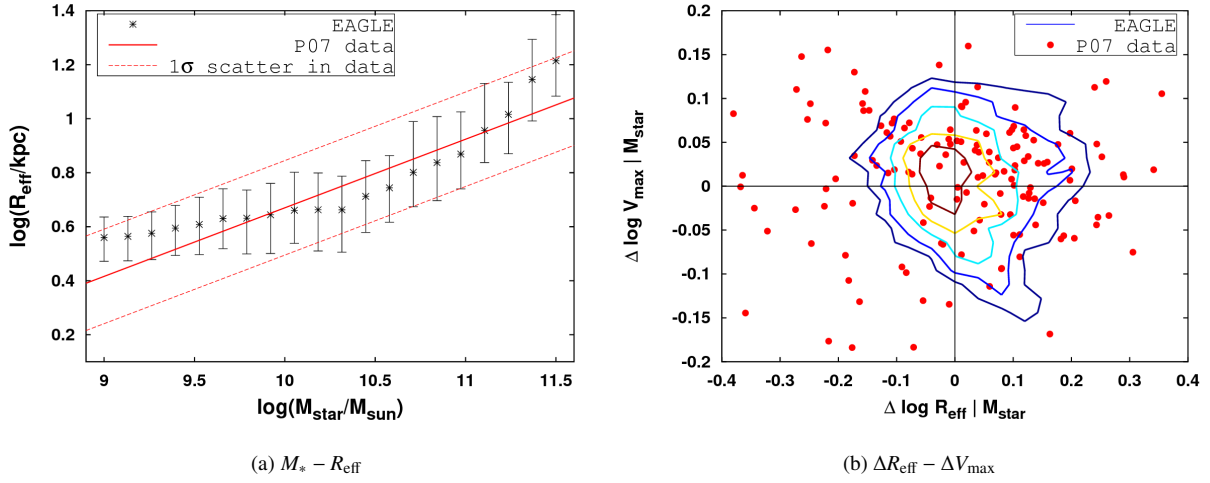


Figure 1. The $M_{\star} - R_{\text{eff}}$ relation and correlation of R_{eff} and V_{max} residuals in the EAGLE simulation, compared to the observations of Pizagno et al. (2007). As in DW15, stellar masses for the latter were taken from the NASA Sloan Atlas. The red lines in the left panel show the best-fitting power-law to the data, and its scatter. In this plot and those that follow, points indicate medians and error bars 16th and 84th percentiles. We stack the 100 mock data sets (Section 2.3) to make contour plots, and the levels enclose 90, 80, 60, 40 and 20 per cent of galaxies. The spread in the sizes of EAGLE galaxies is as low as is observed, and they correctly exhibit no significant $\Delta R_{\text{eff}} - \Delta V_{\text{max}}$ correlation. In Fig. 1b, the observations have $\rho_{\Delta R - \Delta V} = -0.07$, and the EAGLE galaxies have $\rho_{\Delta R - \Delta V} = -0.13$.

	P07	EAGLE	AM	AM+MMW
s_{MSR}	0.18	0.15 ± 0.01	<i>0.18</i>	0.39 ± 0.03
$\rho_{\Delta R - \Delta V}$	-0.07	-0.13 ± 0.07	-0.22 ± 0.04	-0.56 ± 0.05
$\rho_{\Delta R - \Delta M_{\text{DM}}}$	–	0.18 ± 0.07	<i>0</i>	0.75 ± 0.04
$\rho_{\Delta R - \Delta c}$	–	-0.19 ± 0.07	<i>0</i>	-0.76 ± 0.04
$\rho_{\Delta R - \Delta \lambda}$	–	0.17 ± 0.08	<i>0</i>	0.80 ± 0.04

Table 1. Comparison of statistics of the galaxy–halo connection in observations (P07), the EAGLE simulation, an abundance matching model with sizes chosen to match the stellar mass–size relation by construction (“AM”), and an analogous model with sizes set by angular momentum partition (“AM+MMW”; Desmond & Wechsler 2015; see also Section 3.1). s_{MSR} is the scatter in size of the stellar mass–size relation, ρ denotes Spearman rank correlation coefficient, and Δ is defined in Eq. 1. Entries in italics are by construction. The AM+MMW model overpredicts both s_{MSR} and $|\rho_{\Delta R - \Delta V}|$ due to the strong correlations it implies between R_{eff} and M_{DM} , c and λ at fixed M_{\star} . The EAGLE galaxy–halo connection, in which these variables are only weakly correlated, performs significantly better on both statistics.

for two alternative models. In the “AM” model, stellar mass is set by AM (using the V_{peak} proxy and a scatter of 0.2 dex; Reddick et al. 2013), and galaxy sizes are chosen randomly from a normal distribution at given M_{\star} to match the MSR of the P07 data by construction. In the “AM+MMW” model, the sizes of model galaxies are determined by the MMW model after AM has been performed, using the procedure and best-fitting parameter values of DW15.³

As mentioned in Section 1 (and discussed in detail in DW15), the AM+MMW model compares poorly with observations in both s_{MSR} and $\rho_{\Delta R - \Delta V}$. s_{MSR} includes a contribution of around 0.25 dex from λ , and further contributions from the spread in M_{DM} and c at

³ We note that the AM model favoured by DW15 generates a correlation between M_{\star} and c in the same direction as found for EAGLE galaxies in Matthee et al. (2016), and with a comparable $M_{\star} - M_{\text{DM}}$ scatter.

fixed M_{\star} . $\rho_{\Delta R - \Delta V}$ has contributions both from baryonic mass (higher surface density means larger rotation velocity), and from the dark matter, since in the MMW model more concentrated haloes, which generate larger rotation velocities, host smaller galaxies at fixed angular momentum. The AM model, which includes only the baryonic mass contribution, predicts a $\Delta R - \Delta V$ anticorrelation that is weaker but still stronger than the data’s. We now investigate the origin of the difference between the EAGLE and AM+MMW results.

3.2 Comparison of the haloes in the DMO and hydrodynamical runs of the EAGLE simulation

A possible reason for the apparent failure of the AM+MMW model is its application in DW15 to haloes from an N-body simulation in which baryonic effects were neglected. In Figure 2 we show the fractional differences in M_{DM} , c and λ of all matched haloes in the EAGLE DMO and hydro runs, and compare in the insets their overall distributions. We find the haloes to be a few per cent less massive on average in the hydro run, and their c and λ values to be similar. (Schaller et al. 2015 reported larger differences in halo mass because they included baryons as well as dark matter in the mass definition.) The spin distribution is slightly wider in the hydro run, which goes in the wrong direction to account for the lower s_{MSR} in EAGLE than in the AM+MMW model. In addition, we find that the $M_{\text{DM}} - c$ relations of the two runs are similar, and that the effects of baryons on M_{DM} and c are negligibly correlated with M_{\star}/M_{DM} .

In Figure 3 we compare the correlations of λ with M_{DM} and c in the two runs. If spin was more positively correlated with M_{DM} or c with baryonic effects included, then the corresponding increase in rotational velocity caused by dark matter for larger galaxies would compensate for the reduction in the rotation velocity caused by baryons, which could allow the AM+MMW model to achieve agreement with the measured $\rho_{\Delta R - \Delta V}$. We do not find such an increased correlation, however, leading us to conclude that the differences between the EAGLE and AM+MMW models in their predictions for s_{MSR} and $\rho_{\Delta R - \Delta V}$ arise not from the underlying dark

matter halo structure, but rather from differences in the correlations of galaxy and halo variables. It is to these that we turn next.

3.3 The galaxy–halo connection

Rows 3–5 of Table 1 record the Spearman rank coefficients of the correlations between size residual (ΔR_{eff}) and M_{DM} , c and λ residual in the EAGLE, AM, and AM+MMW models. As halo properties cannot be measured in the observations, there are no corresponding entries in the first column. By construction, the AM model does not correlate galaxy size with any halo property at fixed stellar mass. As described in Section 1, however, the AM+MMW model implies a strong correlation of ΔR_{eff} with $\Delta\lambda$ and a strong anticorrelation with Δc , and the latter in particular is responsible for the strongly negative value of $\rho_{\Delta R-\Delta V}$. In the EAGLE simulation, galaxy size correlates only weakly with each halo variable, with the result that the predicted $\rho_{\Delta R-\Delta V}$ is similar to the AM case. In addition, the weakness of these correlations prevents s_{MSR} from receiving the full contributions from the scatter in halo variables at fixed M_* , allowing it to remain below the P07 value.

4 DISCUSSION AND CONCLUSIONS

While the principle component of the galaxy–halo connection – the relation between galaxy mass and halo mass and concentration – is becoming well constrained by abundance matching studies, secondary components, such as the dependence of galaxy size on halo properties, remain uncertain. A leading model for galaxy size (Mo et al. 1998; MMW) assumes proportionality of galaxy and halo specific angular momentum, making galaxy size a specific function of stellar mass and halo mass, concentration and spin. Despite success in matching the normalisation of the stellar mass–size relation when combined with an $M_* - M_{\text{DM}}$ relation from AM, this model overpredicts both the spread in sizes (s_{MSR}) and the strength of the correlation of size and velocity residuals ($\rho_{\Delta R-\Delta V}$). This indicates a problem with the galaxy–halo connection it implies.

In this *Letter*, we investigated this discrepancy in the context of the EAGLE hydrodynamical simulation. We found the galaxy population in this simulation to exhibit near-agreement with measurements of both s_{MSR} and $\rho_{\Delta R-\Delta V}$. We demonstrated that this difference with the AM+MMW prediction is due not to modifications to the haloes themselves due to baryonic effects, but rather to the weakness of the correlations of galaxy size with M_{DM} , c and λ at fixed M_* . While the MMW model strongly correlates galaxy size with dark matter mass ($\rho = 0.75$), halo concentration ($\rho = -0.76$) and halo spin ($\rho = 0.80$) at fixed M_* , the Spearman rank coefficients for the corresponding EAGLE correlations are only 0.18, -0.19 and 0.17, respectively. These values are consistent with 0 within 3σ .

Our results have implications for both galaxy formation theory and semi-analytic and empirical modelling. On one hand, the breakdown of the assumption of angular momentum partition between baryons and dark matter requires explanation. That galaxy and halo spins are only weakly correlated may suggest stochastic transfer of angular momentum between them that scrambles an initial correlation, or a significant loss or redistribution of angular momentum through feedback or cooling processes (Brook et al. 2011; Zjupa & Springel 2016). On the other hand, the EAGLE galaxy–halo correlations measured here may be used to inform semi-empirical models in which galaxy sizes are added by hand. To match s_{MSR} and $\rho_{\Delta R-\Delta V}$, at least in an AM framework, R_{eff} should correlate at most weakly with M_{DM} , c and λ at fixed M_* . This is

tacitly assumed by several existing models (e.g. Dutton et al. 2011, 2013; Desmond & Wechsler 2016), and implied also by aspects of the mass discrepancy–acceleration relation (Desmond 2016). We suggest such correlations be used by default from now on. Finally, our results facilitate the testing of predictive galaxy formation theories: if a theory’s effective galaxy–halo connection exhibits correlations compatible with those of EAGLE, its success in matching the fine-grained statistics that we investigate here is assured.

ACKNOWLEDGEMENTS

We thank Simon Foreman, Yu Lu, and Matthieu Schaller for comments on the manuscript, and Matthieu Schaller for guidance with the EAGLE data. This work received partial support from the U.S. Department of Energy under contract number DE-AC02-76SF00515. This work used the DiRAC Data Centric system at Durham University, operated by the Institute for Computational Cosmology on behalf of the STFC DiRAC HPC Facility (www.dirac.ac.uk). This equipment was funded by a BIS National E-infrastructure capital grant ST/K00042X/1, STFC capital grant ST/K00087X/1, DiRAC Operations grant ST/K003267/1 and Durham University. DiRAC is part of the National E-Infrastructure. This work was supported by the Netherlands Organisation for Scientific Research (NWO), through VICI grant 639.043.409, and the European Research Council under the European Union’s Seventh Framework Programme (FP7/2007–2013) / ERC Grant agreement 278594-GasAroundGalaxies. RAC is a Royal Society University Research Fellow. We are grateful to the computational teams at SLAC and Durham for their support.

REFERENCES

- Behroozi P. S., Conroy C., Wechsler R. H., 2010, ApJ, 717, 379
- Behroozi, P. S., Wechsler, R. H., & Wu, H.-Y. 2013, ApJ, 762, 109
- Brook C. B. et al., 2011, MNRAS, 415, 1051
- de Jong R. S., Lacey C., 2000, ApJ, 545, 781
- Conroy C., Wechsler R. H., Kravtsov A. V., 2006, ApJ, 647, 201
- Courteau S., Dutton A., van den Bosch F. C., MacArthur L. A., Dekel A., McIntosh D. H., Dale D. A., 2007, ApJ, 671, 203
- Crain R. A. et al., 2015, MNRAS, 450, 1937
- Croton D. J. et al., 2006, MNRAS, 365, 11
- Desmond H., Wechsler R. H., 2015, MNRAS, 454, 322
- Desmond H., Wechsler R. H., 2016, MNRAS, preprint (arXiv:1604.04670)
- Desmond H., 2016, MNRAS, 464, 4160
- Dolag K., Borgani S., Murante G., Springel V., 2009, MNRAS, 399, 497
- Dutton A. A., van den Bosch F. C., Dekel A., Courteau S., 2007, ApJ, 654, 27
- Dutton A. A. et al., 2011, MNRAS, 416, 322
- Dutton A. A., Macciò A. V., Mendel J. T., Simard L., 2013, MNRAS, 432, 2496
- Ferrero I. et al., 2016, preprint (arXiv:1607.03100)
- Furlong M. et al., 2016, preprint (arXiv:1510.05645)
- Gnedin O. Y., Weinberg D. H., Pizagno J., Prada F., Rix H.-W., 2007, ApJ, 671, 1115
- Klypin, A., Kravtsov, A. V., Bullock, J. S., & Primack, J. R. 2001, ApJ, 554, 903
- Kravtsov A. V., 2013, ApJL, 764, L31
- Kravtsov A. V., Berlind A. A., Wechsler R. H., Klypin A. A., Gottlöber S., Allgood B., Primack J. R., 2004, ApJ, 609, 35
- Lehmann B. V., Mao Y.-Y., Becker M. R., Skillman S. W., Wechsler R. H., 2015, preprint (arXiv:1510.05651)
- Mo H.J., Mao S., White S.D.M., 1998, MNRAS, 295, 319
- Lu Y., Mo H. J., Weinberg M. D., Katz N., 2011, MNRAS, 416, 1949

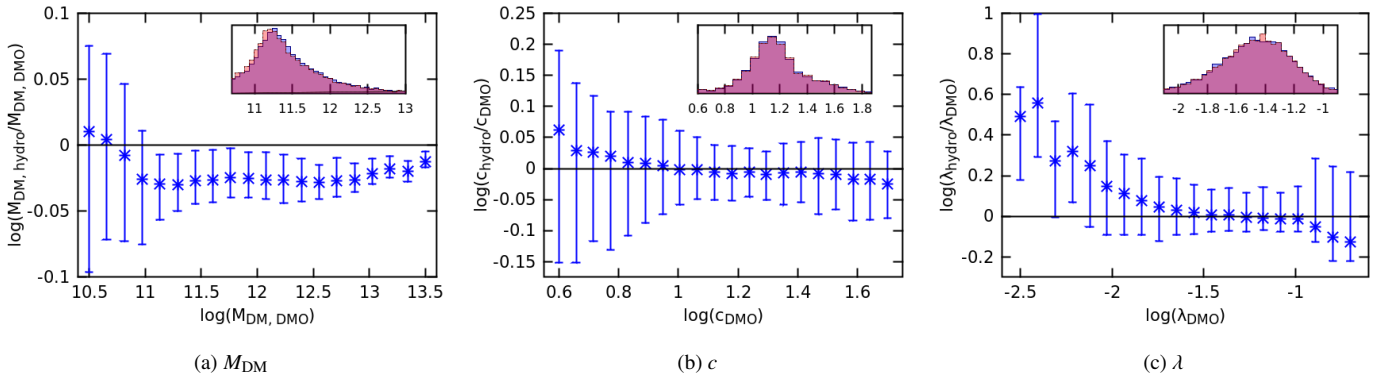


Figure 2. The differences in M_{DM} , c and λ between all $M_* > 10^9 M_{\odot}$ haloes in the hydro runs of the EAGLE simulation and their counterparts in the DMO run, as a function of the DMO variable. The insets compare the overall distributions (hydro in red and DMO in blue). With baryonic effects included, M_{DM} is reduced by a few per cent on average (the catalogue is incomplete for $M_{\text{DM}} \lesssim 10^{11} M_{\odot}$), and λ increased slightly at low values. c is largely unaffected.

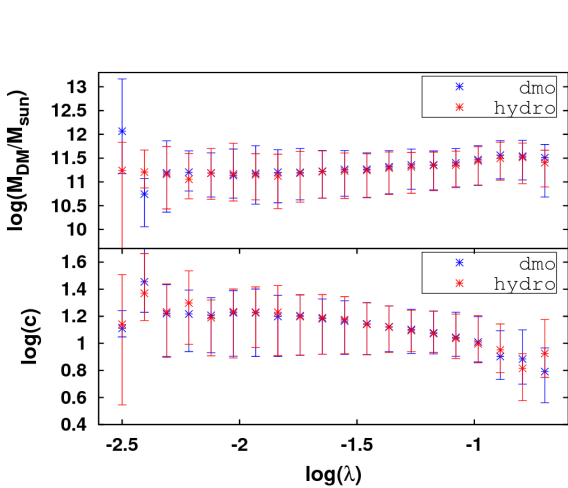


Figure 3. λ correlates in the same way with both M_{DM} and c for $M_* > 10^9 M_{\odot}$ haloes in the DMO and hydro runs of the EAGLE simulation. Together with Fig. 2, this shows that the difference between the EAGLE and AM+MMW models in their predictions for s_{MSR} and $\rho_{\Delta R-\Delta V}$ are not due to changes to the haloes caused by baryons. They must therefore be due to different correlations between galaxy and halo variables.

Lu Y., Mo H. J., Wechsler R. H., 2015, MNRAS, 446, 1907
 Matthee J., Schaye J., Crain R. A., Schaller M., Bower R., Theuns T., 2016, preprint (arXiv:1608.08218)
 McGaugh S. S., 2005, Phys. Rev. Lett., 95, 171302
 Peebles, P. J. E. 1969, ApJ, 155, 393
 Pizagno J. et al., 2007, AJ, 134, 945
 Reddick R. M., Wechsler R. H., Tinker J. L., Behroozi P. S., 2013, ApJ, 771, 30
 Reyes R., Mandelbaum R., Gunn J. E., Pizagno J., Lackner C. N., 2011, MNRAS, 417, 2347
 Sales L. V., Navarro J. F., Schaye J., Dalla Vecchia C., Springel V., Haas M. R., Helmi A., 2009, MNRAS, 399, L64
 Sales L. V. et al., 2012, MNRAS, 423, 1544
 Schaller M. et al., 2015, MNRAS, 451, 1247
 Schaye J. et al., 2015, MNRAS, 446, 521
 Somerville R. S. et al., 2008, ApJ, 672, 776–786
 Springel V., 2005, MNRAS, 364, 1105
 Springel V., White S. D. M., Tormen G., Kauffmann G., 2001, MNRAS,

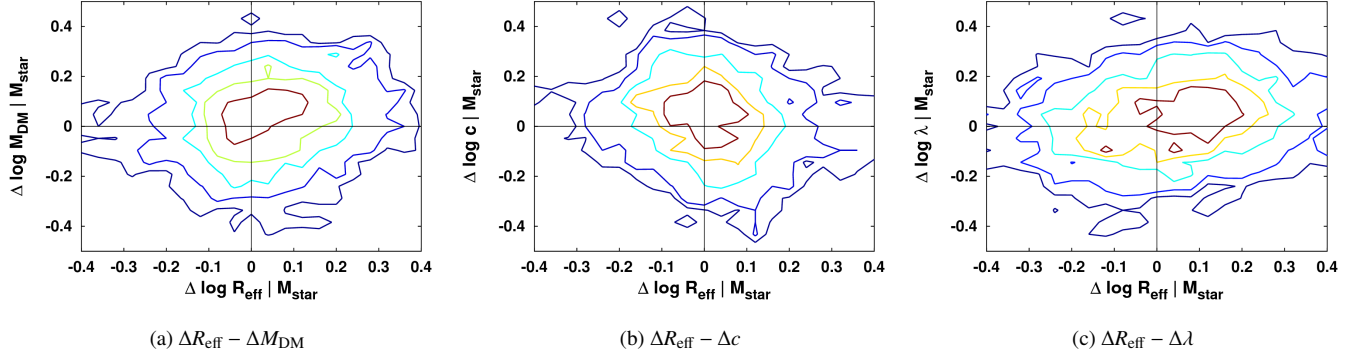


Figure 4. The correlation of residuals of the stellar mass–size relation with dark matter mass, concentration and spin residuals in the hydro run of the EAGLE simulation. Haloes were randomly selected from the catalogue to reproduce the stellar mass distribution of the P07 sample (see Section 2.3). In contrast to the AM+MMW model, EAGLE predicts these correlations to be weak, which accounts for the better agreement of the predicted s_{MSR} and $\rho_{\Delta R - \Delta V}$ values with the observations. The Spearman rank correlation coefficients of these relations are 0.18, −0.19 and 0.17, respectively (see Table 1).